04

Self-diffraction of light waves at contra-directional mixing in the cubic photorefractive crystal of 23 symmetry class

© V.N. Naunyka, A.V. Makarevich

Mozyr State Pedagogical University named after I.P.Shamyakin, Mozyr, Republic of Belarus

e-mail: valnav@inbox.ru

Received June 11, 2023
Revised July 19, 2023
Accepted July 24, 2023

Regularities of the influence of self-diffraction of the light waves on the energy transfer in the case of contra-directional two-wave mixing in the cubic photorefractive piezocrystal of 23 symmetry class are analyzed. The dependence of the relative intensity of the object wave on the azimuth of its polarization and the orientation angle of the photorefractive crystal is theoretically and experimentally investigated. It is shown that when solving the equations of coupled waves without taking into account self-diffraction, the most accurate estimate of the intensity of the object wave at the output of the crystal is achieved in the case when the vector amplitudes of linearly polarized mixing waves in the crystal bulk belong to the same plane. In the general case, for arbitrary values of the azimuth of the linear polarization of the object wave and the orientation angle of the crystal, neglection of self-diffraction of light waves by formed reflection holographic grating at calculations can lead to the significant disagreements between results of theoretical calculation in comparison with experimental data.

Keywords: Two-wave mixing, photorefractive crystal, hologram, self-diffraction, coupled wave equations.

DOI: 10.61011/EOS.2023.08.57286.5308-23

Introduction

Due to the unique combination of high photosensitivity and the ability to operate in real time, photorefractive crystalline materials are used to develop a variety of devices for the information photonics, such as adaptive holographic interferometers, optical modulators, interference and diffraction filters, as well as devices based on them (see, for example, [1]). In recent years, a number of studies have been published [2–4], describing new directions for the practical application of photorefractive crystals. The possibility of using $Bi_{12}SiO_{20}$ (BSO) and CdTe crystals as photosensitive media in optical radiation detectors for positron emission tomography was demonstrated in [2]. In [3] it is shown that the $LiNbO_3:Fe$ photorefractive crystal can be successfully used in holographic encryption and decryption systems. The study presents the results of testing a holographic decryption system in terms of displacement of the phase key both in the longitudinal and transverse directions from the original position, as well as blind decryption without knowing the correct key. An analysis of the possibilities of using the photorefractive effect in neuromorphic computing in telecommunication applications is given in [4].

The nonlinear optical effect, which consists in the self-action of light beams in the recording medium as a result of changes in its properties under the influence of induced radiation, was predicted in early studies [5–7] and plays an important role in the formation of dynamic holograms in photorefractive crystals [8,9]. The self-action of light beams when recording a hologram in a dynamic recording medium results in the situation that the light beams recording the holographic grating are subjected to diffraction by this grating [8]. This causes a change in the intensity and phase of the recording beams and affects the further process of formation of the hologram [6,8]. The described wave phenomenon was named self-diffraction of light [5].

The influence of self-diffraction on the properties of bulk holographic gratings in a dynamic recording medium has been studied by a number of authors (see, for example, [5,6,8]). A generalization of the well-known Kogelnik's theory of coupled waves [10] to the case of bulk holograms formed in absorbing photosensitive media taking into account the self-diffraction of light beams was proposed in [11]. The study presents an analytical asymptotic solution to differential equations with variable coefficients, on the basis of which the amplitudes of diffracted coupled waves can be found. Using the yielded expressions, the properties of transmission and reflection holograms in the presence of absorption by a photosensitive medium were studied. The resulting analytical expressions were taken into account in [12] to analyze the influence of local and non-local nonlinearities of the medium on the diffraction efficiency of a hologram recorded in a photorefractive crystal. It is shown that the self-diffraction of recording light waves affects the selective properties of holographic gratings: not only the half-width of the Bragg peak changes but also a shift in the maxima occurs on the graphs of the diffraction efficiency of transmission and reflection holograms as function of the thickness of the recording medium and the magnitude of the phase mismatch.

In cubic photorefractive crystals, modulation of the dielectric constant at optical frequencies, apart from the

linear electro-optical effect, can be additionally due to the photoelastic and inverse piezoelectric effects [13]. At the same time, non-centrosymmetric cubic photorefractive crystals also have noticeable optical activity [14]. As shown in [15], the combined action of optical activity, photoelastic and piezoelectric effects causes significant changes in the polarization and energy characteristics of the reconstructed wave that arises as a result of the reference beam diffraction by the bulk hologram recorded in the crystal. In [15], the theory of light diffraction by a phase holographic grating formed in a cubic optically active photorefractive piezocrystal is presented. The influence of photoelasticity on the self-diffraction of light waves by a bulk hologram in a non-centrosymmetric photorefractive crystal of 23 symmetry class was studied in [16]. It has been established that a necessary condition for consistency of the results of theoretical calculations and the obtained experimental data is to take into account the contribution of photoelastic and piezoelectric effects in the equations of coupled waves used to describe the mixing of the reference and object light beams on a holographic grating. In [17], the self-diffraction of mixing waves by a transmission hologram in a BSO crystal was studied and the conditions for achieving the highest values of the relative intensity of the object light wave were established.

Features of self-diffraction of light by a bulk holographic grating in a photorefractive crystal of $43m$ symmetry class are analyzed in [18,19]. In [18], the possibility of non-unidirectional energy transfer between coupled waves is shown when their polarization state changes due to the mixing. In a linear approximation based on the modulation coefficient of the induced interference pattern, analytical expressions are obtained for finding the scalar amplitudes of the components of the reference and object light waves. In [19], an exact solution to the equations of coupled waves was obtained, on the basis of which the amplitudes of arbitrarily polarized light beams can be found during their mixing on a transmission hologram formed in a photorefractive crystal of $\bar{4}3m$ symmetry class.

As can be seen from the above review of studies, the effect of self-diffraction of light waves on the properties of interaction holograms in cubic photorefractive crystals has been studied by a number of authors. At the same time, features of the energy exchange during counter-propagating two-wave mixing in a cubic photorefractive crystal taking into account the mutual influence of recording light beams and the formed reflection hologram, are almost unstudied (a review of publications on the properties of reflection holograms is given in [20]). Therefore, for the purpose of effective practical application of cubic photorefractive crystals, it is of interest to determine the conditions of a holographic experiment (azimuths of linear polarization of waves at the entrance to the crystal, orientation angle of the crystal, etc.), under which the self-diffraction effect has the greatest influence on the energy exchange between coupled waves during their contra-directional mixing on a reflection hologram. It is also important to determine the limits of

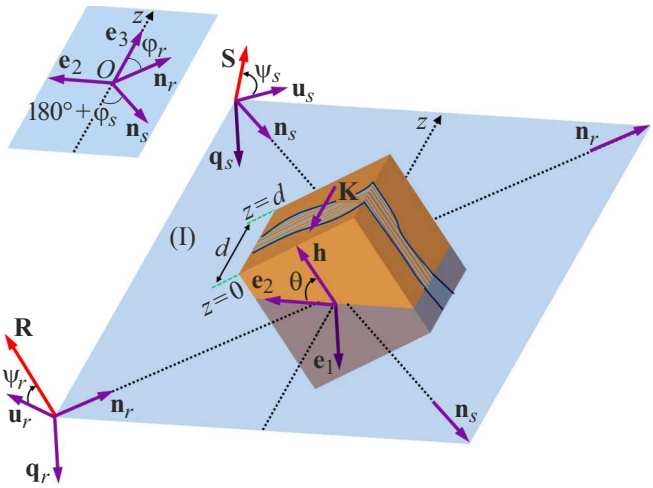

Figure 1. Schematic diagram of contra-directional mixing of two light waves in a photorefractive crystal.

applicability of the analytical expressions presented in [21], which are obtained in the approximation of a given (static) grating for finding the amplitude of an object wave during contra-directional two-wave mixing. Solving these problems will make it possible to more accurately predict the results of holographic experiments and improve the efficiency of the use of cubic photorefractive crystals as light-sensitive media in devices for recording, processing, and transmitting optical information.

Thus, the purpose of this study is to analyze the patterns of self-diffraction of light waves during degenerate contra-directional two-wave mixing in the cubic photorefractive crystal of 23 symmetry class. The results of the theoretical analysis presented in the study were obtained based on the numerical solving coupled wave equations, which take into account the linear electro-optical, photoelastic, and inverse piezoelectric effects, and also the optical activity, natural absorption, and circular dichroism of the crystal are taken into account. To verify the results obtained theoretically, an experimental investigation of the dependence of the relative intensity of the object light wave on the orientation angle of the (001) cut BSO crystal was carried out at various azimuths of the linear polarization of light waves.

Theoretical model

Let two plane monochromatic linearly polarized light waves be directed at a cubic photorefractive crystal of 23 symmetry class: the reference (subscript — r) wave and the object wave (subscript — s) (Fig. 1). When building up a theoretical model, triples of unit vectors $(\mathbf{q}_r, \mathbf{u}_r, \mathbf{n}_r)$ and $(\mathbf{q}_s, \mathbf{u}_s, \mathbf{n}_s)$ are used to specify the polarization state and direction of wave propagation. Wave normals of the reference and object waves coincide in direction with the unit vectors $\mathbf{n}_r$ and $\mathbf{n}_s$. Vector amplitudes $\mathbf{R}$ and $\mathbf{S}$ are perpendicular to vectors $\mathbf{n}_r$ and $\mathbf{n}_s$. Angles ψ_r and ψ_s

define polarization azimuths of the reference and object waves, which are measured from vectors $\mathbf{u}_r$ and $\mathbf{u}_s$ to vector amplitudes $\mathbf{R}$ and $\mathbf{S}$ clockwise when looking in the direction of vectors $\mathbf{n}_r$ and $\mathbf{n}_s$, respectively.

The orthogonal basis $\mathbf{e}_1, \mathbf{e}_2, \mathbf{e}_3$ is rigidly connected to plane (I), which is parallel to the plane of the holographic table (vector $\mathbf{e}_3$ enters the crystal and is shown in the inset on the left in Fig. 1). Unit vectors $\mathbf{e}_2$ and $\mathbf{e}_3$ lie in plane (I), and vector $\mathbf{e}_1$ is perpendicular to it. Along the Oz axis, which coincides in direction with the vector $\mathbf{e}_3$, the thickness of the crystal d is measured. Assume the crystal faces exposed to the light beams are covered with an antireflection coating, and the effect of waves formed during reflection from them can be neglected. The unit vector $\mathbf{h}$ is rigidly connected to the crystallographic coordinate system and is used to specify the orientation of the crystal relative to the plane of the holographic table. The crystal can be rotated relative to the Oz axis by an orientation angle θ, which is formed by vectors $\mathbf{e}_2$ and $\mathbf{h}$. Bragg angles φ_r, φ_s are measured in plane (I) and are determined by the angular distances between the unit vector $\mathbf{e}_3$ and vectors $\mathbf{n}_r, \mathbf{n}_s$, respectively (see inset to Fig. 1).

In the case of contra-directional mixing of waves in the crystal, a phase reflection hologram is formed with a wave vector $\mathbf{K}$ with its direction opposite to the direction of axis Oz. In Fig. 1, parallel lines applied to the crystal show the periodically located phase planes of the hologram, scattering the wavefronts.

From the wave equation for optically active media in the approximation of slowly varying amplitudes, a well-known (see, for example, [22]) system of equations of coupled waves is obtained, which can be used to describe the mixing of two linearly polarized light waves in the reflection geometry in the photorefractive crystal:

$$\frac{dR_1}{dz} = ie^{-i\delta}\kappa_{r1s1}S_1 + ie^{-i\delta}\kappa_{r1s2}S_2 + \rho_r R_2 - \alpha_r R_1, \quad (1)$$

$$\frac{dR_2}{dz} = ie^{-i\delta}\kappa_{r2s1}S_1 + ie^{-i\delta}\kappa_{r2s2}S_2 - \rho_r R_1 - \alpha_r R_2, \quad (2)$$

$$\frac{dS_1}{dz} = ie^{i\delta}\kappa_{s1r1}R_1 + ie^{i\delta}\kappa_{s1r2}R_2 + \rho_s S_2 - \alpha_s S_1, \quad (3)$$

$$\frac{dS_2}{dz} = ie^{i\delta}\kappa_{s2r1}R_1 + ie^{i\delta}\kappa_{s2r2}R_2 - \rho_s S_1 - \alpha_s S_2. \quad (4)$$

Expressions (1)–(4) use the following notation: R_1, R_2, S_1, S_2 are projections of vector amplitudes $\mathbf{R}$ and $\mathbf{S}$ on the axes that coincide in direction with the unit vectors $\mathbf{q}_r, \mathbf{u}_r, \mathbf{q}_s$ and $\mathbf{u}_s$, respectively; δ is phase shift between the fringe pattern and the holographic grating; $\rho_{r,s} = (\rho + i\chi)/\cos\varphi_{r,s}$ is specific rotation of the plane of polarization of the reference and object waves, ρ is optical activity parameter, χ is circular dichroism coefficient; $\alpha_{r,s} = \alpha/\cos\varphi_{r,s}$ is parameter used to set the absorption of the reference and object waves, α is absorption coefficient of the crystal; i is imaginary unit. The coupling coefficients κ_{uhqt} between the reference and object waves propagating in the crystal are found on the basis of the following relationships: $\kappa_{uhqt} = -\kappa_0(\mathbf{e}^*_{uh}\Delta\hat{\varepsilon}^{-1}\mathbf{e}_{qt})/\cos\varphi_u$, where $\kappa_0 = \pi n^3/(2\lambda)$, n is refraction index of the unperturbed crystal, λ is wavelength; $u, q = r, s$; $h, t = 1, 2$. The mutual coupling between the components of vector amplitudes of the reference and object waves during their contra-directional mixing in the cubic photorefractive crystal is specified by means of tensor convolutions $(\mathbf{e}^*_{uh}\Delta\hat{\varepsilon}^{-1}\mathbf{e}_{qt})$, where $\Delta\hat{\varepsilon}^{-1}$ are changes in the components of the inverse dielectric constant tensor, which can be found based on the well-known expression $\Delta\hat{\varepsilon}^{-1} = (r^S_{vwp}n_p + p^S_{vwkl}n_l\gamma_{ki}e_{pif}n_p n_f)E_{sc}$ [23]. This expression uses the following notation: r^S_{vwp} and p^S_{vwkl} are tensor components of the linear electro-optical $(\hat{r}^S)$ and photoelastic $(\hat{p}^E)$ effects, respectively; γ_{ki} are components of the tensor inverse to the tensor $\Gamma_{ik} = C^E_{ijkl}n_j n_l$, where C^E_{ijkl} are components of the elastic modulus tensor $(\hat{c}^E)$; e_{pif} are tensor components of the inverse piezoelectric $(\hat{e})$ effect; $\mathbf{E}_{sc} = mE_{sc}\mathbf{n}$, where E_{sc} is modulus of the electric field strength of the holographic grating, m is modulation depth of the fringe pattern, which is found from the following expression: $m = 2(R_1S_1 + R_2S_2\cos(\mathbf{u}_s\mathbf{u}_r))/\left(R_1^2 + R_2^2 + S_1^2 + S_2^2\right)$; n_p, n_f are direction cosines of vector $\mathbf{n}$ in the crystallographic coordinate system. Superscript S for the linear electro-optical effect tensor $\hat{r}^S$ means that its components were measured for a clamped crystal. Superscript E for the tensors $\hat{p}^E, \hat{c}^E$ means that the components of the elasticity and photoelastic effect tensors were measured with a constant electric field. In the case of non-zero components of the tensors $\hat{r}^S$, $\hat{p}^E$, $\hat{c}^E$ and $\hat{e}$, which were obtained for a cubic crystal of 23 symmetry class, the following notation is adopted in the text below:

$$r^S_{123} = r^S_{132} = r^S_{213} = r^S_{231} = r^S_{312} = r^S_{321} \equiv r_{41},$$

$$p^E_{11} = p^E_{22} = p^E_{33} \equiv p_1, \quad p^E_{12} = p^E_{23} = p^E_{31} \equiv p_2,$$

$$p^E_{13} = p^E_{21} = p^E_{32} \equiv p_3, \quad p^E_{44} = p^E_{55} = p^E_{66} \equiv p_4,$$

$$e_{123} = e_{132} = e_{213} = e_{231} = e_{312} = e_{321} \equiv e_{14},$$

$$c^E_{11} = c^E_{22} = c^E_{33} \equiv c_1,$$

$$c^E_{12} = c^E_{13} = c^E_{23} = c^E_{21} = c^E_{31} = c^E_{32} \equiv c_2,$$

$$c^E_{44} = c^E_{55} = c^E_{66} \equiv c_3.$$

In further calculations, a medium with the following BSO crystal parameters was selected: the refraction index of the unperturbed crystal is $n_0 = 2.54$ at $\lambda = 633 \cdot 10^{-9}$ m [8]; the electro-optical coefficient is $r_{41} = 5 \cdot 10^{-12}$ m/V [8]; the elasticity coefficients are $c_1 = 12.96 \cdot 10^{10}$ N/m^2, $c_2 = 2.99 \cdot 10^{10}$ N/m^2, $c_3 = 2.45 \cdot 10^{10}$ N/m^2 [24]; the photoelasticity coefficients are $p_1 = -0.16$, $p_2 = -0.13$, $p_3 = -0.12$, $p_4 = -0.015$ [25]; the piezoelectric coefficient is $e_{14} = 1.12$ C/m^2 [25].

Equations of coupled waves (1)–(4) were numerically integrated on the basis of the well-known shooting method [26]. The initial conditions for solving the two-point

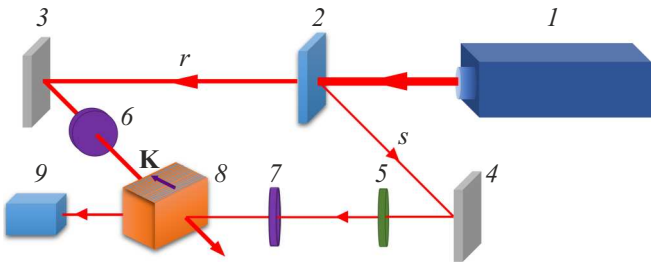

Figure 2. Schematic diagram of the experimental setup: *1* — helium-neon laser, *2* — light beam splitter; *3, 4* — totally reflecting mirrors; *5* — phase half-wave plate; *6, 7* — orifice plates; *8* — crystal; *9* — photodiode.

boundary value problem were chosen as follows: for $z = 0$ it is assumed that $R_1 = -|\mathbf{R}| \sin\psi_r$, $R_2 = |\mathbf{R}| \cos\psi_r$; for $z = d$ it is assumed that $S_1 = -|\mathbf{S}| \sin\psi_s$, $S_2 = |\mathbf{S}| \cos\psi_s$. A quantitative assessment of the energy exchange between coupled waves was made using the relative intensity parameter γ of the object wave, which was found by the following formula: $\gamma = I_S/I_S^0$. Here I_s denotes the intensity of the object wave during two-wave mixing in reflection geometry (Fig. 1), which is fixed at the exit from the crystal (at $z = 0$). The parameter I_s^0 is equal to the intensity of the object wave at the exit from the crystal in the absence of the reference wave.

Experimental

Let us consider the experimental scheme (Fig. 2) of contra-directional two-wave mixing in a photorefractive crystal, which was used to verify the theoretical results presented below. Helium-neon laser *1* generated radiation at a wavelength of 632.8 nm, which was divided into two light beams using beam splitter *2*. The reference light beam linearly polarized in the plane of incidence (r) was reflected from totally reflecting mirror *3*, passed through orifice *6* and was directed to the crystal. The object (s) light beam, after reflection from totally reflecting mirror *4*, was passed through half-wave phase plate *5* and after passing through orifice *7* it was directed to the crystal. As a result of the mixing of the reference and object beams in the photorefractive crystal, a reflection hologram with a wave vector $\mathbf{K}$ was formed. To record the intensity of the object beam, photodiode *9* was used, which was located along the path of propagation of this beam. The photodiode was connected to a measuring circuit (not shown in Fig. 2) containing a digital voltmeter, the readings of which were recorded and the ratio $\gamma = I_S/I_S^0$ was determined based on the data obtained.

When performing the experiments, we used the holographic experiment technique described in [27]. Initially, the crystal was rotated relative to the z axis and the required orientation angle θ was set. Then, the reference beam was blocked, and only the object beam was directed onto the crystal and its intensity I_s^0 was measured. After this, the light-sensitive area of photodiode *9* was shielded with an opaque screen, and the crystal was continuously illuminated by the reference and object beams for 30 s. Then, the opaque screen located in front of the photosensitive area of photodiode *9* was removed and the intensity of the object beam I_s during contra-directional two-wave mixing was recorded using a digital voltmeter. Then, the orientation angle θ of the crystal was changed, and the described sequence of actions of the experiment was repeated.

To perform the experiment, a (001) cut sample with a thickness of 3.73 mm was selected from the available BSO crystals. The choice of cut and thickness of the crystalline sample was made in accordance with the data given in [28]. The authors have shown that for a BSO crystal with a thickness of up to 10 mm, the highest values of the relative intensity of the object wave with an appropriate choice of input azimuths of linear polarization of light waves are achieved if the wave vector of the reflection hologram is directed along one of crystallographic directions of the ⟨100⟩ family. It was also established in the study that the graph of the highest relative intensity of the object wave as a function of the crystalline sample thickness during contra-directional two-wave mixing in a (001) cut BSO crystal achieves its maxima if the following condition is met: $d_g \approx g\pi/(2\rho)$ $(g = 1, 3, \ldots)$. Due to the fact that the experimentally measured specific rotation of available BSO samples was approximately equal to $\rho = 384$ rad/m, the minimum thickness at which the largest value γ could be achieved was $d_1 \approx 4.21$ mm. The BSO sample with a thickness of 3.73 mm had the closest value to d_1.

Before conducting the experiment on contra-directional two-wave mixing, the following parameters of the selected BSO crystal were approximately assessed experimentally: natural absorption $\alpha = 15\,\mathrm{m}^{-1}$, circular dichroism $\chi = 1.5\,\mathrm{m}^{-1}$. When preparing the holographic experiment, the φ_r and φ_s angles were chosen equal to 2.5 and 177.5°, respectively, and the ratio of the intensities of the reference and object light beams was 6 : 1. When measuring the θ angle, it was assumed that the unit vector $\mathbf{h}$ was oriented along the crystallographic direction [100].

Results and discussion

Fig. 3 shows a graph of the dependence of the relative intensity γ of the object light wave on the azimuth ψ_s, specified at $z = d$, and the orientation angle θ . The surface $\gamma(\theta, \psi_s)$ is calculated in the approximation of a given grating $(m = \mathrm{const})$ provided that the reference wave is linearly polarized in the plane of incidence. The origin point of azimuth ψ_s was chosen to be 98° because in this case, due to optical activity, vector amplitudes $\mathbf{R}$ and $\mathbf{S}$ of coupled waves during their propagation in the crystal remain in the same plane ($\mathbf{R} \parallel \mathbf{S}$) for any fixed value of the crystal's thickness [29]. In the case of a change in the azimuth ψ_s during the propagation of coupled waves inside the crystal,

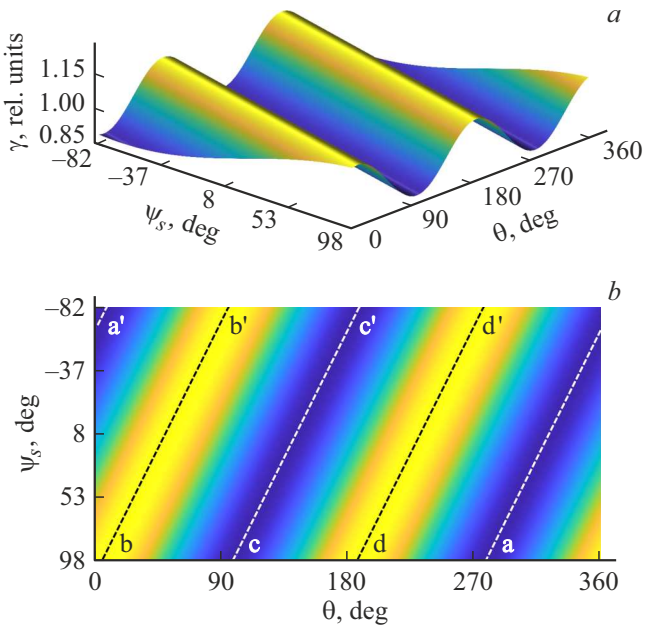

Figure 3. Graph of the relative intensity γ of the object wave as a function of the orientation angle θ and polarization azimuth ψ_s, calculated in the approximation of a given grating.

an angle of $\Delta = |98^\circ - \psi_s|$, appears between the vector amplitudes **R** and **S**, which is kept for any value of z. For example, with $\psi_s = 8^\circ$ vectors **R** and **S** are perpendicular to each other ($\mathbf{R} \perp \mathbf{S}$) for any coordinate z, because $\Delta = 90^\circ$.

As can be seen from Fig. 3, the graph of $\gamma(\theta, \psi_s)$, obtained from numerical solving the equations of coupled waves (1)–(4) without taking into account self-diffraction (in the approximation of a given grating), has a wave-like form with clearly visible lines of maxima and minima (shown with dashed lines in Fig. 3, *b*). In this case, each value of angle θ can be associated with a value of azimuth ψ_s at which the relative intensity γ will achieve its maximum. It has also been established that the highest intensity of the object wave takes place when the orientation angle changes in the ranges from 4 to 94° (line $b-b'$) and from 184 to 274° (line $d-d'$). The smallest values of γ on the surface $\gamma(\theta, \psi_s)$ are achieved along the dashed lines $a-a'$ and $c-c'$, which correspond to the following intervals of change of the angle θ: 0–4° and 274–360° ($a-a'$); 94–184° ($c-c'$). In particular, the relative intensity γ remains constant in magnitude if the values of azimuth ψ_s and angle θ are related by a linear dependence: $\psi_s = 98^\circ + \theta$.

Fig. 4 shows a graph of the dependence $\gamma(\theta, \psi_s)$, which was obtained by taking into account the self-diffraction of light waves by the reflection hologram recorded in the crystal. To take into account the effect of self-diffraction when solving the coupled wave equations (1)–(4), a dynamic approximation was used. Within the framework of this approximation, it was assumed that during the experiment, the recording fringe pattern and the holographic grating in the photorefractive crystal achieve a certain mutually consistent state. In the linear recording mode, the amplitude of the holographic grating is proportional to the modulation depth m of the recording fringe pattern, which, in contrast to the approximation of a given grating, is a function of z coordinate ($m(z) \neq \text{const}$) inside the crystal [6].

When numerically solving the equations of coupled waves (1)–(4), the „inclusion“ of self-diffraction causes mainly a qualitative transformation of the $\gamma(\theta, \psi_s)$ graph: in the dynamic approximation the surface becomes hump-shaped with symmetrically located global maxima (points A and C) and global minima (points B and D). As can be seen from Fig. 4, when recording a reflection hologram in dynamic mode, all extrema of the $\gamma(\theta, \psi_s)$ graph correspond to one value of azimuth, ψ_s, and two different values of the orientation angle. In the case we have considered, this azimuth value ψ_s is approximately equal to 94°, and the angle values θ, at which the maxima and minima of the surface are achieved, are equal to 4° (point A), 184° (point C), and 94° (point B), 274° (point D), respectively. As the azimuth ψ_s decreases, the energy exchange between light waves becomes weaker, and the amplitude of relative intensity fluctuations γ with a change in angle θ decreases. In the limiting case, when the azimuth ψ_s is in the vicinity of -4° (dashed line $e - e'$ in Fig. 3, *b*), the relative intensity γ will have values close to unity. This means the absence of energy exchange between the reference and object waves during their contra-directional mixing. With a further decrease in the value of

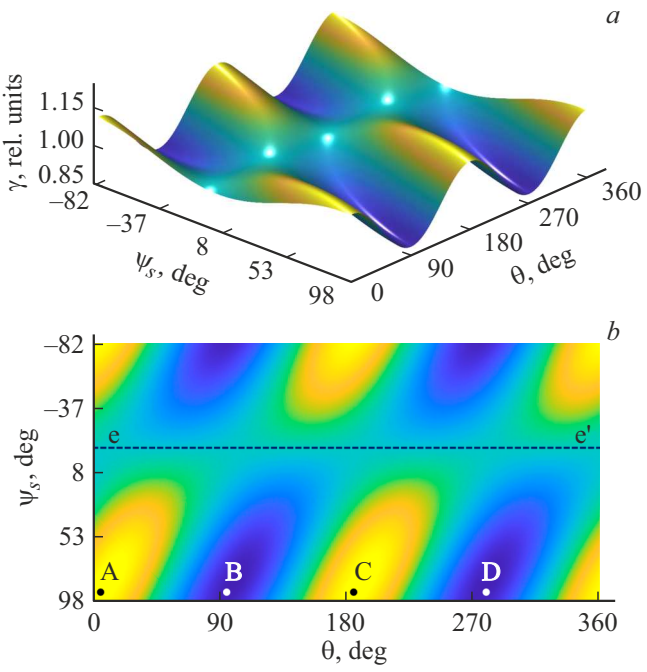

Figure 4. Graph of the dependence of the relative intensity γ of the object wave on the orientation angle θ and polarization azimuth ψ_s, calculated in the dynamic approximation.

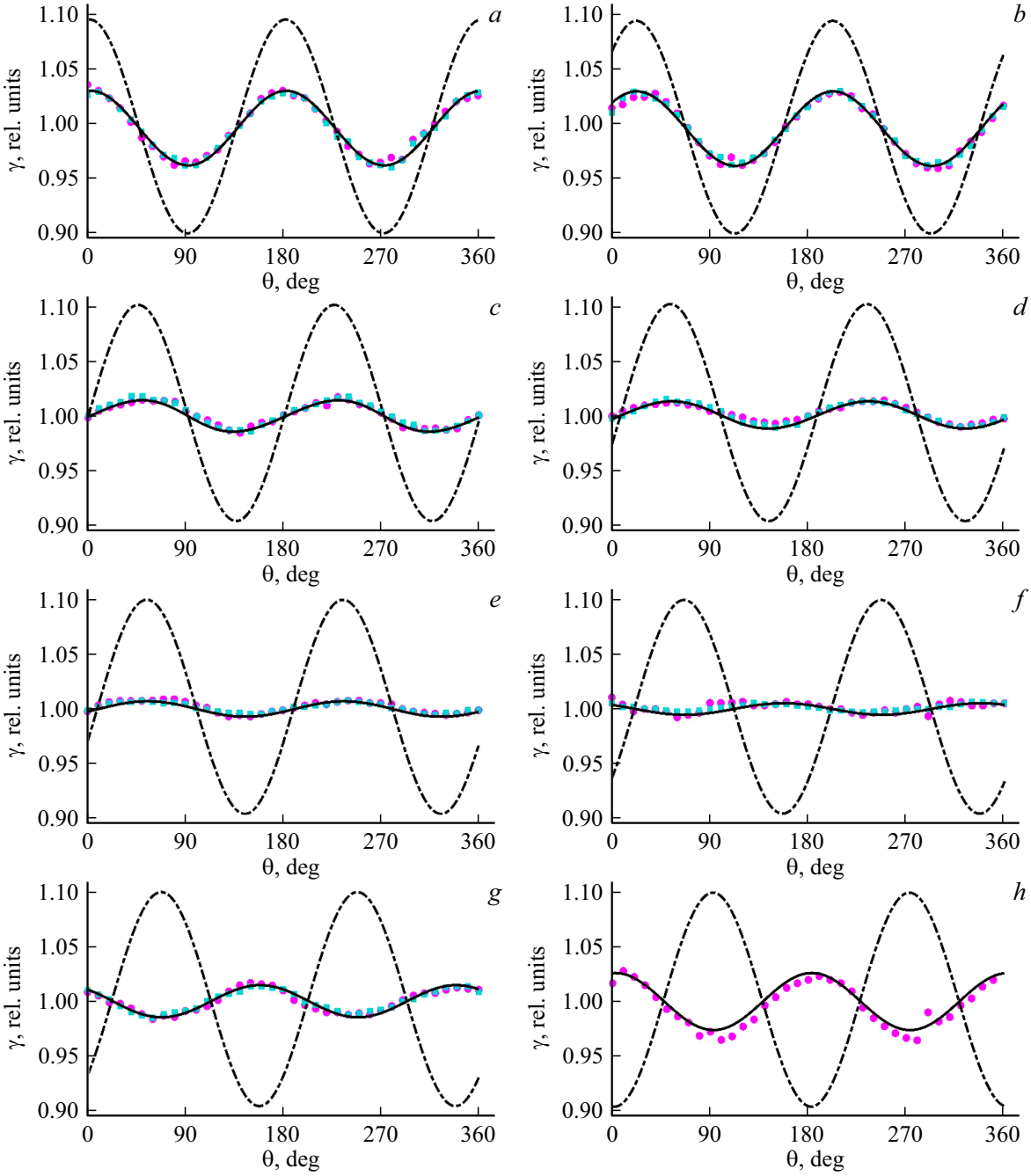

Figure 5. Graphs of the dependence of the relative intensity γ of the object wave on the orientation angle θ, obtained experimentally and theoretically for different values of the polarization azimuth ψ_s: $\psi_s = 98^\circ$ (*a*); $\psi_s = 53^\circ$ (*b*); $\psi_s = 8^\circ$ (*c*); $\psi_s = 3^\circ$ (*d*); $\psi_s = -7^\circ$ (*e*); $\psi_s = -22^\circ$ (*f*); $\psi_s = -37^\circ$ (*g*); $\psi_s = -82^\circ$ (*h*).

the polarization azimuth ($\psi_s \to -82^\circ$), two local maxima and minima are again formed on the $\gamma(\theta, \psi_s)$ surface.

As can be seen from a comparison between Fig. 3 and 4, there are fundamental qualitative differences in the graphs of $\gamma(\theta, \psi_s)$, calculated with and without taking into account the self-action of light waves when recording a reflection hologram in a photorefractive (001) cut BSO crystal. The key question here is the following: is it possible to achieve a maximum relative intensity γ for any angle θ with an appropriate choice of azimuth ψ_s, as predicted by the solution to coupled wave equations (1)–(4) in the approximation of a given grating, or there are only a few combinations of values (θ, ψ_s) at which the parameter γ achieves extreme values as it is obtained in the dynamic approximation. In addition, it is important to answer the question: whether or not there are such values of azimuth ψ_s for which at any value of the angle θ the relative intensity γ has a value close to unity. In the approximation of a given grating,

there are no such values of the object wave polarization azimuth — for any azimuth ψ_s the relative intensity γ changes periodically with a corresponding change in the angle θ. The results of the numerical solving the equations of coupled waves (1)–(4) in the dynamic approximation show that there is a value of azimuth ψ_s, in the vicinity of which $\gamma \approx 1$. To verify the correctness of the application of the two above theoretical approaches to describing the $\gamma(\theta, \psi_s)$, the dependence of the relative intensity γ on the orientation angle θ was studied experimentally for different values of the polarization azimuth ψ_s.

Fig. 5 shows graphs of the dependence of the relative intensity γ of the object light wave on the angle θ, obtained for different azimuth values ψ_s. The dash-dot lines show the $\gamma(\theta)$ dependences obtained in the approximation of a given grating and correspond to sections of the $\gamma(\theta, \psi_s)$ surface shown in Fig. 3 by planes $\psi_s = \text{const}$. The solid curves in Fig. 5 represent the $\gamma(\theta)$ dependences obtained in the dynamic approximation, which coincide with the sections of the $\gamma(\theta, \psi_s)$ surface shown in Fig. 4 by planes $\psi_s = \text{const}$. The graphs of dependences shown with circles and squares are the data from two series of holographic experiments. A small shift (of the order of a few degrees) of the maxima of the $\gamma(\theta, \psi_s)$ graphs in Fig. 3, 4 and $\gamma(\theta)$ graphs in Fig. 5 relative to the origin of the orientation angle ($\theta = 0^\circ$) is due to the fact that in the BSO crystalline sample used, the direction of the crystallographic axis [100] was known with an error of a few degrees. Due to this situation the adjustment of the crystal in the experimental setup could not be started exactly from the [100] axis, which led to an insignificant shift of the above-mentioned graphs relative to each other.

The curves in Fig. 5, *a* were calculated for $\psi_s \approx 98^\circ$, which corresponds to the case when **R** and **S** vector amplitudes for contra-directional propagation of light waves inside the crystal are in the same plane. In this figure, the theoretical and experimental curves are qualitatively similar to each other, however the graph of $\gamma(\theta)$ calculated in the dynamic approximation is quantitatively more accurately corresponds to the experimental data. As the angle Δ between vector amplitudes **R** and **S** inside the crystal increases, the theoretical and experimental curves shift by an angle of θ, which is equal to half the angle between these vectors ($\Delta/2$). For example, with $\psi_s \approx 53^\circ$ (Fig. 5, *b*) the angle Δ between vector amplitudes **R** and **S** is equal to 45°, and the shift of the maxima took place approximately by 22°, or, for example, with $\Delta = 90^\circ$ a shift in the dependence graphs is achieved, approximately equal to 45° (Fig. 5, *c*).

As the experimental data presented in Fig. 5 show, the highest values of relative intensity γ can be achieved only in the case when the input polarization azimuths are chosen in such a way that the vector amplitudes **R** and **S** are in the same plane. With increasing angle Δ the relative intensities γ decrease at the maxima of the graph of $\gamma(\theta)$. For example, if at $\psi_s \approx 98^\circ$ ($\Delta = 0^\circ$) the parameter γ is approximately equal to 1.03 (Fig. 5, *a*), then at $\psi_s \approx 53^\circ$ ($\Delta = 45^\circ$) the $\gamma \approx 1.025$ is obtained (Fig. 5, *b*), and at $\psi_s \approx 8^\circ$ ($\Delta = 90^\circ$) this parameter is $\gamma \approx 1.015$ (Fig. 5, *c*). When the azimuth ψ_s varying in the range from 8° (Fig. 5, *c*) to −37° (Fig. 5, *g*), the relative intensity γ takes values close to unity, and the graph of $\gamma(\theta)$ changes qualitatively — as the azimuth ψ_s decreases, the maxima and minima of the graph of $\gamma(\theta)$ exchange places: in the intervals of θ that corresponded to maxima of the $\gamma(\theta)$ dependence minima are formed, and vice versa. The change-over of maxima and minima on the graph of $\gamma(\theta)$ is clearly visible if we compare the curves in Fig. 5, *c* and 5, *g*.

For a more detailed experimental study of the curve transformation with azimuth ψ_s varying in the range from 8 to −37°, additional experiments were carried out to study the $\gamma(\theta)$ dependence at $\psi_s \approx 3^\circ$ (Fig. 5, *d*), −7° (Fig. 5, *e*), and −22° (fig. 5, *f*). It can be seen from the presented experimental data, how with azimuth ψ_s decreasing in the interval under study the curve $\gamma(\theta)$ transforms from a wave-like dependence (Fig. 5, *c*) to a close-to-linear dependence (Fig. 5, *f*) and then to an „inverted“ wave-like curve (Fig. 5, *g*).

The experimentally studied transformation of the $\gamma(\theta)$ graph with decreasing azimuth ψ_s cannot be satisfactorily described within the framework of the approximation of a given grating, because the set of experimental data presented in Fig. 5 does not correspond to the surface shown in Fig. 3. The best qualitative agreement between the theoretical data obtained by solving the equations of coupled waves (1)–(4) in the approximation of a given grating with the experimental results is achieved only in the case when the vector amplitudes **R** and **S** inside the crystal are in the same plane. As can be seen from Fig. 5, in the general case, only the self-diffraction of light waves taken into account in calculations makes it possible to achieve good agreement between the experimental data and the theoretically calculated graphs of the $\gamma(\theta)$ dependence. It has been experimentally established that there are two combinations of θ, ψ_s at which the parameter γ achieves its maximum on the $\gamma(\theta, \psi_s)$ surface, which corresponds to the theoretical data obtained from solving the equations of coupled waves (1)–(4) in the dynamic approximation. It has also been experimentally proven that there are azimuths ψ_s at which the relative intensity γ is approximately equal to unity for any angle θ, which is predicted as a result of solving the problem taking into account the self-diffraction effect.

Conclusion

It has been experimentally proven that the highest values of the relative intensity of the object wave during contra-directional two-wave mixing in a (001) cut BSO crystal can be achieved by choosing such values of the azimuths of linear polarization of light waves at which their vector amplitudes inside the crystal are in the same plane. In this case, there are only two combinations of values of the polarization azimuth of the object wave and the orientation

angle of the crystal at which the absolute maximum of the relative intensity of the object wave can be achieved. When experimentally determining the relative intensity of an object wave, the existence of such azimuths of its polarization was discovered for which the energy exchange between the coupled waves is nearly stopped at any orientation angle of the BSO crystal.

Also, when studying the dependence of the relative intensity of an object wave on its polarization azimuth and crystal orientation angle, it was established that solving the equations of coupled waves in the approximation of a given grating, in the general case, leads to incorrect results. The most accurate predictions of the $\gamma(\theta)$ dependence when performing numerical calculations without taking into account the self-diffraction are achieved for the case when the vector amplitudes of light waves inside the crystal are in the same plane. In other cases, when estimating the intensity of an object wave, an error may arise, which is due to the neglect of the effect of the mutual influence of coupled waves and the holographic grating on each other.

Thus, the self-diffraction has a significant effect on the direction and intensity of energy exchange between light waves during their contra-directional mixing in the cubic photorefractive crystal of 23 symmetry class. Solving the equations of coupled waves in the dynamic approximation makes it possible to achieve the most accurate agreement between the graphs of the relative intensity of the object wave dependence on its polarization azimuth and the orientation angle of the crystal and the obtained experimental data.

Funding

The study was financially supported by the Ministry of Education of the Republic of Belarus (agreement dated March 22, 2021 № 1410/2021) within the State Program of Scientific Research № 6 „Photonics and electronics for innovations“ for 2021−2025. (assignment 6.1.14).

Conflict of interest

The authors declare that they have no conflict of interest.

References

[1] V.M. Petrov, A.V. Shamray, *Interferentsiya i diffraktsiya dlya interferentsionnoy fotoniki* (Lan, SPb., 2019), 460 p. (in Russian).
[2] L. Tao, H.M. Daghighian, C.S. Levin. J. Medical Imaging, **4** (1), 011010 (2017). DOI: 10.1117/1.JMI.4.1.011010
[3] C.H. Kwak, G.Y. Kim, B. Javidi. Opt. Commun., **95**, 437 (2019). DOI: 10.1016/j.optcom.2018.12.049
[4] F. Laporte, J. Dambre, P. Bienstman. Scientific Reports, **11**, 2701 (2021). DOI: 10.1038/s41598-021-81899-w
[5] V.M. Komissarov, Pisma v ZhETF,**14**, 64 (1971) (in Russian).
[6] V.L. Vinetsky, N.V. Kukhtarev, S.G. Odulov, M.S. Soskin, UFN, **129** (1), 8 (1979) (in Russian).
[7] B.Ya. Zeldovich, V.V. Shkunov, T.V. Yakovleva, UFN, **149** (3), 511 (1986) (in Russian).
[8] M.P. Petrov, S.I. Stepanov, A.V. Khomenko, *Fotorefraktivnye kristally v kogerentnoy optike* (Nauka, SPb, 1992), 320 p. (in Russian).
[9] S.G. Odulov, M.S. Soskin, A.I. Khizhnyak, *Lazery na dinamicheskikh reshetkakh: opticheskie generatory na chetyrekhvolnovom smeshenii* (Nauka, M., 1990), 272 p. (in Russian).
[10] H. Kogelnik. JOSA, **57** (3), 431 (1967).
[11] V.M. Serdyuk, ZhTF, **58** (7), 1341 (1988) (in Russian).
[12] V.M. Serdyuk, ZhTF, **59** (10), 11 (1989) (in Russian).
[13] A.A. Izvanov, A.E. Mandel, N.D. Khatkov, S.M. Shandarov, Avtometriya, **2**, 79 (1986) (in Russian).
[14] A.A. Blistanov, V.S. Bondarenko, N.V. Perelomova, F.N. Strizhevskaya, V.V. Chkalova, M.P. Shaskolskaya, *Akusticheskie kristally* (Nauka, M., 1982), 632 p. (in Russian).
[15] V.V. Shepelevich, S.M. Shandarov, A.E. Mandel. Ferroelectrics, **110**, 235 (1990).
[16] V.I. Volkov, Yu.F. Kargin, N.V. Kukhtarev, A.V. Privalko, T.I. Semenets, S.M. Shandarov, V.V. Shepelevich. Sov. J. Quantum Electron., **21** (10), 1122 (1991). DOI: 10.1070/QE1991v021n10ABEH004302.
[17] V.V. Shepelevich, A.A. Firsov. Quantum Electron., **30** (1), 60 (2000). DOI: 10.1070/QE20 00v030n01ABEH001659.
[18] R.V. Litvinov. JETP, **95** (5), 820 (2002). DOI: 10.1070/QE2002v032n06ABEH002238.
[19] R.V. Litvinov. Quantum Electron., **37** (2), 154 (2007). DOI: 10.1070/QE2007v037n02ABEH013349.
[20] S.M. Shandarov, N.I. Burimov, Yu.N. Kul'chin, R.V. Romashko, A.L. Tolstik, V.V. Shepelevich. Quantum Electron., **38** (11), 1059 (2008). DOI: 10.1070/QE2008v038n11ABEH013793.
[21] V.V. Shepelevich, V.N. Navnyko, S.F. Nichiporko, S.M. Shandarov, A.E. Mandel'. Tech. Phys. Lett., **29** (9), 757 (2003). DOI: 10.1134/1.1615557.
[22] V.N. Naunyka, V.V. Shepelevich, S.M. Shandarov. Opt. Spectrosc., **129** (1), 84 (2021). DOI: 10.1134/S0030400X21010148.
[23] S.M. Shandarov, V.V. Shepelevich, N.D. Khatkov. Opt. Spectrosc., **70** (5), 627 (1991).
[24] K.S. Aleksandrov, V.S. Bondarenko, M.P. Zaitseva, B.P. Sorokin, Yu.I. Kokorin, V.M. Zrazhevsky, A.M. Sysoev, B.V. Sobolev, FTT, **26** (12), 3603 (1984) (in Russian).
[25] E.I. Leonov, G.A. Babonas, A.A. Reza, V.I. Shandaris, ZhTF, **55** (6), 1203 (1985) (in Russian).
[26] Y.H. Ja. Opt. and Quant. Electron., **15**, 529 (1983).
[27] V.V. Shepelevich, N.N. Egorov, Pisma v ZhTF, **17** (5), 24 (1991) (in Russian).
[28] V.N. Naunyka, V.V. Shepelevich. Tech. Phys. Lett., **33** (9), 726 (2007). DOI: 10.1134/s1063785007090039.
[29] S. Mallick, M. Miteva, L. Nikolova. JOSA B, **14** (5), 1179 (1997). DOI: 10.1364/JOSAB.14.001179.

Translated by Y.Alekseev